MECHANISM OF MOTION OF AN OPTICAL FIBER ALIGNED BY A SOLDER DROPLET

Adam Powell, James Warren and Christopher Bailey*
National Institute of Standards and Technology, Gaithersburg, Maryland, USA
*University of Greenwich, Department of Computing and Mathematical Sciences, London, UK

ABSTRACT

Solder is often used as an adhesive to attach optical fibers to a circuit board. In this proceeding we will discuss efforts to model the motion of an optical fiber during the wetting and solidification of the adhesive solder droplet. The extent of motion is determined by several competing forces, during three "stages" of solder joint formation. First, capillary forces of the liquid phase control the fiber position. Second, during solidification, the presence of the liquid-solid-vapor triple line as well as a reduced liquid solder volume leads to a change in the net capillary force on the optical fiber. Finally, the solidification front itself impinges on the fiber. Publicly-available finite element models are used to calculate the time-dependent position of the solidification front and shape of the free surface.

INTRODUCTION

With the increased use of optical fibers for communications has come a need for a robust means of joining fibers to a substrate and device. Narrow core high-bandwidth fiber requires extremely tight fiber-device alignment tolerances to prevent drastic signal reduction. For applications in harsh environments, a small droplet of solder is often used to hold the fiber in alignment with a device. The fiber is positioned to maximize optical performance of the device, and then the solder preform next to the fiber is melted so that it flows across the pad and over the fiber. Solder joint geometry considered here is shown in figure 1.

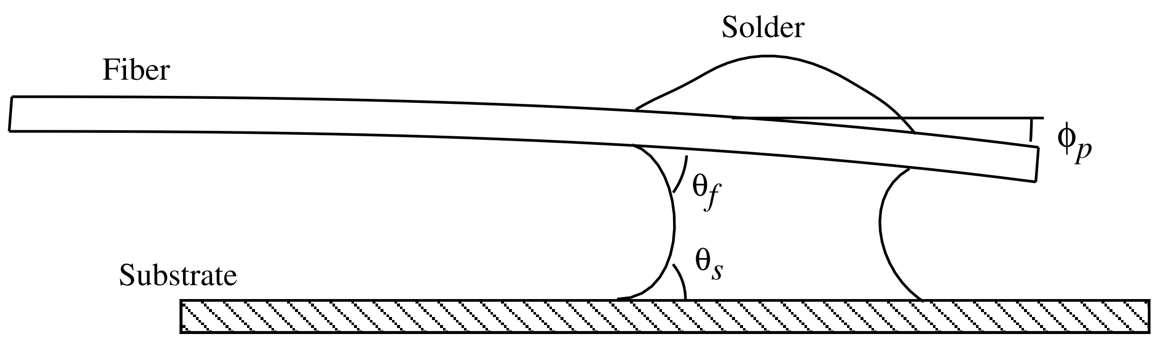

Figure 1: Geometry of the solder joint used to align an optical fiber. θ_f and θ_s are solder contact angles on the fiber and substrate, and ϕ_p is the angle at which a deflected fiber passes through the solder droplet. (Not to scale.)

Unfortunately, during the melting and solidification of the solder, significant motion of the fiber is observed to occur, decreasing the transmission efficiency. Because the capillary force on the fiber scales as its diameter and its stiffness as its diameter cubed, a very thin fiber is likely to be significantly deflected by the capillary force. Furthermore, as the solder joint solidifies, its volume changes, and with it the shape of the liquid surface and the magnitude of the capillary force on the fiber. Finally, as the solidified solder makes contact with the fiber, the shrinkage during cooling pulls the fiber further out of alignment.

In order to solve this problem, after the fiber is positioned for maximum transmission, it is offset to compensate for estimated shift, with some improvement in fiber-device collinearity. Here it is hoped that mathematical modeling will bring about an understanding of the problem which will lead to more robust design and less shift, to enable use of higher-bandwidth fiber with tighter collinearity tolerances than are currently achievable.

METHODOLOGY

Fiber shift due to capillary force in liquid solder and solder shrinkage during solidification and cooling were calculated independently, using the public domain programs Surface Evolver and PHYSICA respectively.

Liquid solder capillary force

While the solder droplet is molten, the force on the fiber is assumed to arise from surface tension and hydrostatic pressure in the liquid solder. These forces are determined by the shape of the solder-fiber-air triple line as described in the appendix, which in turn depends on the shape of the solder droplet. The droplet is assumed to reach its minimum-energy shape, which is calculated using the Surface Evolver program written by Ken Brakke [1, 2]. This program moves the surface to minimize the total energy of the system, including energies corresponding to the solder-air, solder-fiber, and solder-substrate surfaces, and also the pressure energy. Gravitational energy is neglected here due to the small droplet size. Surface Evolver creates a triangular mesh of the relevant surfaces, and moves the vertices of the mesh down the gradient of total system energy while maintaining constant solder volume and satisfying geometrical constraints. It also handles all mesh refinement and equiangulation, so the program output is the Delaunay triangulation of a very close approximation to the minimum-energy shape at the specified resolution.

A dimensionless formulation is employed with parameters as shown in table I. Dimensionless parameters are given in reference to the lengthscale L equal to half of the true pad width, and the solder-air surface energy γ, so that for example, the true fiber radius is $0.1L$ and the true modulus is $E\gamma/L$.

Table I: Dimensionless parameters used in Evolver calculations

Parameter	Symbol	Value
Pad length and width		2
Fiber radius	R	0.1
Solder droplet volume		1
Solder-fiber surface energy	γ_{SF}	$\cos(50°)$
Solder-pad surface energy	γ_{SS}	$\cos(30°)$
Fiber modulus	E	10^7
Fiber fixed end–droplet center distance	D	7.3
Fiber free end–droplet center distance		5.8

The region of the substrate outside of the square contact pad is taken to be perfectly non-wetting, so the contact angle of the solder is equal to 30° on the corners, and greater than 30° along the edges where the droplet is constrained by the edge of the pad.

Elastic energy in the fiber

The deformed fiber shape is approximated by a circular arc with elastic energy E_e given by

$$E_e = \frac{\pi E R^4 (\phi_p^2 + \phi_y^2)}{8D} \tag{1}$$

where ϕ_p and ϕ_y are the "pitch" (normal to the substrate) and "yaw" (parallel to the substrate) fiber bending angles respectively.

A Surface Evolver script was written to move the fiber to its equilibrium position where solder capillary and fiber elastic forces balance. Run once every 30 Evolver iterations, this script was a Newton's method root finder which set equal the forces given by derivatives of equation 1 and the appendix. The derivative of capillary force with respect to ϕ_p and ϕ_y was calculated by a central difference method.

Solidification and cooling shrinkage

The heat transfer and solid mechanics model describing fiber motion during and after solidification was based on the PHYSICA package developed at the University of Greenwich [3], and employed a methodology similar to that described by Bailey and Wheeler [5]. To generate the mesh, the triangulated solder-air surface generated by Surface Evolver and meshes generated for the fiber surface and a portion of the substrate were filled with points on a regular lattice. The quickhull algorithm [4] was then used to find the Delaunay tetrahedra which make up the convex hull of those points. Tetrahedra outside of the original surface were eliminated and interior points moved to promote a more uniform tetrahedron volume distribution. These tetrahedra were then used as the volume mesh required by PHYSICA.

In a model problem, the fiber was given as a 25 μm diameter rod, the substrate as a 400×400 μm square of 50 μm thickness with a 125×125 μm square wetting patch at the center.

MODEL RESULTS

Capillary forces

Figure 2 shows the dimensionless capillary force on a perfectly rigid fiber parallel to the substrate as a function of fiber position for a set of dimensionless parameters given in the top section of table I. Dimensionless force given in that figure would be multiplied by γL to give the true force. These calculations show that for this pad geometry and parameter set, the horizontal "aligning" component of the force is a small fraction of the vertical component, so the fiber will bend toward the substrate.

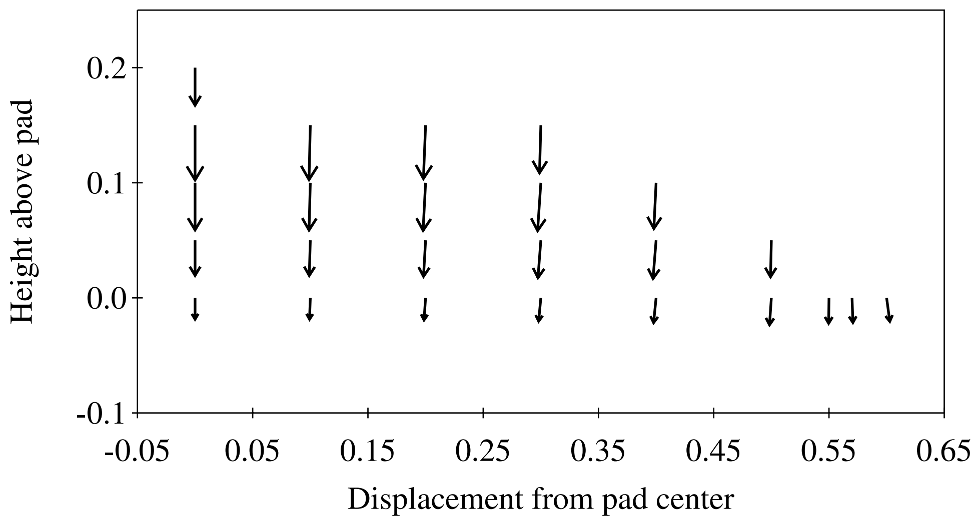

Figure 2: Dimensionless capillary force directions and relative magnitudes exerted on a perfectly rigid fiber as a function of fiber position for the system as described by parameters in the top section of table I. The maximum dimensionless force magnitude is 0.151. The fiber is assumed to be aligned parallel to the pad, and height is measured from the fiber axis to the substrate pad.

When the fiber is allowed to bend, the extent of fiber deflection due to capillary force (calculated within Surface Evolver as described above) is significant. For the conditions given in table I, deflection at the free end reaches a maximum of 0.103, which is more than half the fiber diameter. Figure 3 shows the solder surface under such conditions.

For the parameters given here, fiber diameter has the largest effect on displacement: when the diameter increases from 0.2 to 0.3, the maximum deflection falls to just 0.0044, which is 1.5% of the diameter. This is because the elastic energy (equation 1) is considerably more dependent on the fiber diameter than the surface energy.

Solidification and cooling

PHYSICA results for solid fraction and von Mises stress at different times in the simulation are shown in figure 4. In this case, the initial and boundary conditions resulted in freezing from the substrate upward,

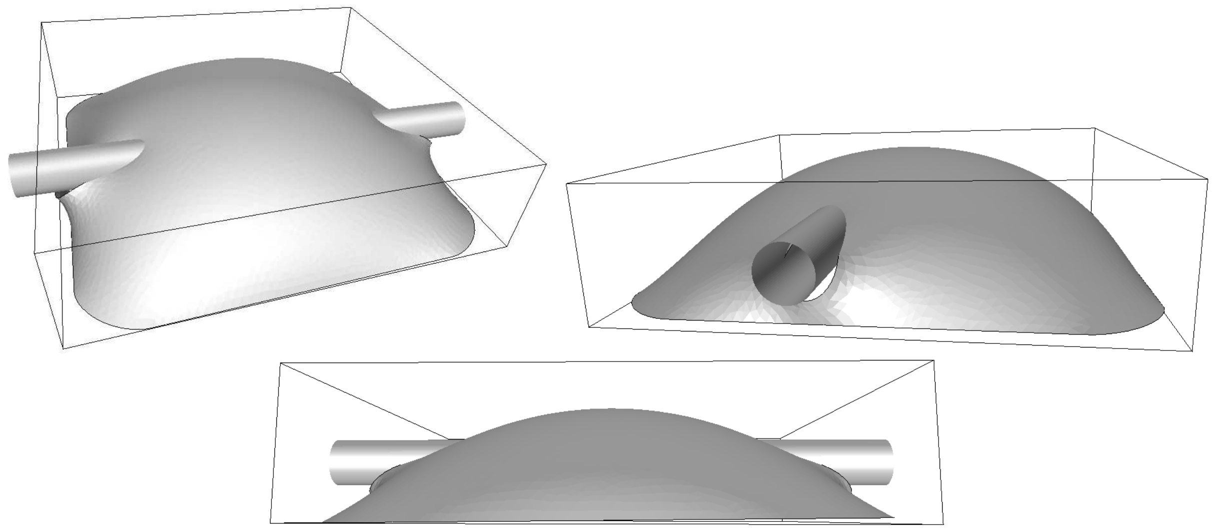

Figure 3: Three views of the calculated solder surface shape around a fiber pulled out of alignment by capillary forces. The grey cylinder shows the original fiber position, and the box is aligned with the fiber to show the angle of fiber deflection relative to the substrate.

and for some time all of the solder was between its liquidus and solidus temperatures.

It is interesting to note that for this geometry and set of material properties, shrinkage in the solder droplet resulted in sufficient deformation of the substrate for the fiber end to move *away* from the substrate. This is because the substrate material was specified to have low thermal expansion coefficient and stiffness relative to the solder, and the substrate was specified to be very thin. The largest stresses were found in the fiber, since maximum strain there is close to that in the solder but the fiber modulus is considerably larger.

CONCLUSIONS

A methodology for calculating the extent of fiber shift during wetting, solidification and cooling of an adhesive solder droplet has been developed based on freely available modeling software tools. As expected, the shift is very sensitive to changes in fiber radius. Also worth noting is that it is possible for solidification shrinkage in the solder to lead to a fiber shift away from the substrate by means of elastic deformation of the substrate.

ACKNOWLEDGMENTS

The authors would like to thank Daniel Wheeler of the University of Greenwich and Mark Beranek of the Boeing Company for many contributions to this project. This work was performed in part under a Co-operative Research and Development Agreement with the NIST ATP Precision Optoelectronics Assembly Consortium, Cooperative Agreement 70NANB5H1092.

Appendix: Capillary Force

At any given point on the fiber-liquid solder-vapor triple line, the local capillary force $\vec{F}$ has magnitude equal to the surface tension γ, and direction perpendicular to the triple line tangent vector $\vec{d\ell}$. The total force on the fiber is equal to the integral of this quantity around both loops of the triple line TL, so that

$$\vec{F}_{total} = \oint_{TL} \vec{F} d\ell. \tag{2}$$

The local capillary force vector $\vec{F}$ satisfies the following constraints:

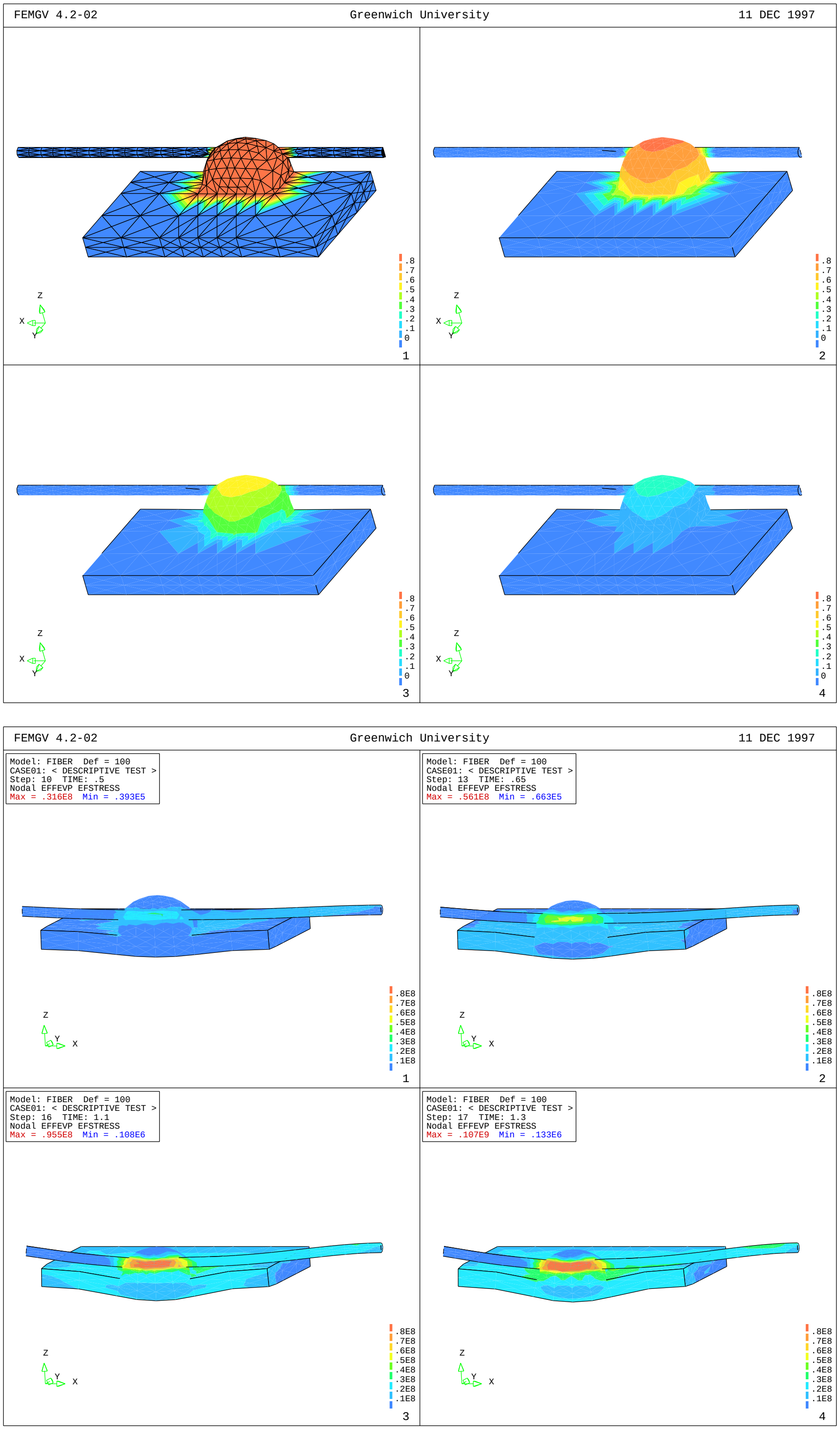

Figure 4: Solid fractions (top) and von Mises stresses (bottom) predicted by PHYSICA at various time steps. Note stress plots are given for a later time than solid fractions, and the mesh is deformed by 100 times the calculated deformation field.

1. It is at an angle θ (the contact angle) to the fiber tangent surface, so $\vec{F} \cdot \hat{n} = \gamma \sin\theta$ where $\hat{n}$ is the outward fiber surface normal of unit length.
2. It is perpendicular to edge tangent vector $\vec{d\ell}$, so $\vec{F} \cdot \vec{d\ell} = 0$.
3. Its magnitude $|\vec{F}|$ is γ, the surface tension.
4. With the edge integral making a clockwise loop around the fiber, the solder droplet is always on the left, so for $\theta < 90°$, $\hat{n} \times \vec{F} \cdot \vec{d\ell} > 0$ (< 0 for $\theta > 90°$).

In cylindrical coordinates transformed so the fiber centerline is the z-axis, its surface will be defined by $r = R$, so $\hat{r}$ can be used as the surface normal $\hat{n}$. Based on this, we can rewrite the first three above conditions for $\vec{F}$ as three simultaneous equations for the three components of $\vec{F}$ as follows:

$$F_r = \gamma \sin\theta \tag{3}$$

$$F_\phi d\ell_\phi + F_z d\ell_z = 0 \tag{4}$$

$$F_r^2 + F_\phi^2 + F_z^2 = \gamma. \tag{5}$$

(Note that $\vec{d\ell}$ has no r-component.) We then substitute 3 into 5, and 4 into 5, and solve for F_ϕ^2 and F_z^2 to give

$$F_\phi^2 = \frac{\gamma^2 \cos^2\theta d\ell_z^2}{d\ell_\phi^2 + d\ell_z^2},\ F_z^2 = \frac{\gamma^2 \cos^2\theta d\ell_\phi}{d\ell_\phi^2 + d\ell_z^2} \tag{6}$$

which simplify, satisfying condition 4, to

$$F_\phi = \frac{\gamma \cos\theta d\ell_z}{|\vec{d\ell}|},\ F_z = -\frac{\gamma \cos\theta d\ell_\phi}{|\vec{d\ell}|}. \tag{7}$$

The components of $\vec{F}$ given by equations 3 and 7 are integrated using equation 2 to give the capillary force on the fiber.

Appendix: Liquid Solder Hydrostatic Pressure

For a small droplet, the surface curvature is high enough that the hydrostatic pressure is significantly higher in the liquid than in the surrounding vapor. The Surface Evolver calculates this pressure as the Lagrange multiplier of the volume constraint, and the components of force exerted on the fiber by this pressure are found by multiplying the pressure by the area bounded by the projection of the triple line in each dimension. For example, the force in the y-direction is given by

$$\vec{F} = P \oint_{TL} z\hat{x} \cdot \vec{d\ell} \tag{8}$$

where $\hat{x}$ is the unit vector in the x-direction.

REFERENCES

1. L.M. Racz, J. Szekely and K.A. Brakke, ISIJ Int'l. **33**, 2 (1993).
2. L.M. Racz and J. Szekely, ISIJ Int'l. **33**, 2 (1993).
3. M Cross, P Chow, C Bailey, N Croft, J Ewer, P Leggett, K McManus, K A Pericleous and M K Patel, Proc. ICIAM 95, July 1995.
4. Barber, C.B., Dobkin, D.P., and Huhdanpaa, H.T., ACM Trans. Math. Software, **22**, 469 (1996).
5. D Wheeler, C,. Bailey, M Cross, Jnl. Manufac. Engineering, Proc Instn Mech Engrs, **212B**, 141 (1998).

6